

Photoinduced phase transitions and lattice deformation in 2D NbOX₂ (X=Cl, Br, I)

Carmel Dansou¹, Charles Paillard^{1,2}, Laurent Bellaïche^{1,3}

¹ *Smart Ferroic Materials center, Institute for Nanosciences & Engineering and Department of Physics, University of Arkansas, Fayetteville AR 72701, USA.*

² *Université Paris-Saclay, CentraleSupélec, CNRS, Laboratoire SPMS, 91190 Gif-sur-Yvette, France. and*

³ *Department of Materials Science and Engineering, Tel Aviv University, Ramat Aviv, Tel Aviv 6997801, Israel.*

(Dated: March 24, 2025)

We present a comprehensive investigation of light-induced phase transitions and strain in two-dimensional NbOX₂ (X = Cl, Br, I) using first-principles calculations. In particular, we identify a light-induced ferroelectric-to-paraelectric phase transition in these 2D systems. Furthermore, we demonstrate the possibility of inducing an antiferroelectric-to-paraelectric transition under illumination. Additionally, we find that these 2D systems exhibit significant photostrictive behavior, adding a new functionality to their already notable optical properties. The ability to control and manipulate ferroelectric order in these nanoscale materials through external stimuli, such as light, holds considerable promise for the development of next-generation electronic and optoelectronic devices.

I. INTRODUCTION

The discovery of materials capable of changing shape in response to external stimuli, such as piezoelectrics and piezomagnets, has led to the development of actuators, micro-electromechanical systems, and microrobotics [1–4]. Like piezoelectricity and piezomagnetism, photostriction [5, 6]—a phenomenon in which light induces mechanical strain in a material—enables to use light as an external handle for next-generation wireless and remote-controlled devices [7, 8]. Consequently, in the last decade, intensive research has been conducted to understand photostriction and new functional materials such as ferroelectrics [9–13], multiferroics [14–19], organic polymers [20], inorganic semiconductors [21] and halide perovskites [22–24].

The niobium oxide dihalides family, NbOX₂ (X = Cl, Br, I), has recently gained a lot of attention as a new class of layered FE materials [25–28] with potential applications as quantum light sources [29] and sensors thanks to their tunable bandgap, monolayer-like excitonic behavior even in bulk form [30], and efficient second-harmonic generation (SHG) response [31]. Moreover, NbOCl₂ has been reported to possess high carrier mobility [32] and strong light absorption in the visible range [33], making it a promising material for optoelectronic applications. Recent studies have also shown that epitaxial strain can significantly enhance the electro-optic behavior of both 2D and 3D NbOI₂ [34].

Motivated by these observations of light-matter coupling in two-dimensional NbOX₂ (X = Cl, Br, I), we employed Density Functional Theory (DFT) calculations to investigate the possibility of inducing phase transition using optical excitation as well as light-induced strains in the NbOX₂ family. Through systematic simulation of optical excitation in the paraelectric (PE), ferroelectric (FE), and antiferroelectric (AFE) phases of 2D-dimensional NbOX₂, we show that a FE-PE transition as well as an AFE-PE transition can be opti-

cally induced. Additionally, we predict that 2D NbOX₂ structures exhibit remarkable photostrictive properties, therefore showing their potential application in light-controlled devices.

II. METHODS AND GROUND STATE STRUCTURES

In this study, DFT calculations were performed using the open-source code Abinit [35]. Optimized Norm-Conserving Vanderbilt pseudopotentials [36] are employed in our simulations. To approximate the exchange-correlation energy, we used the generalized gradient approximation proposed by Perdew, Burke, and Ernzerhof (PBE) [37]. A plane wave cut-off energy of 40 Hartree was used for the three structures, and integration over the Brillouin zone was performed using a non-shifted $6 \times 12 \times 1$ k-mesh. The density during self-consistent field (SCF) calculations was considered converged when the residual forces on the structure were smaller than 10^{-6} Ha.Bohr⁻¹. Single layer NbOX₂ was simulated in the present study. To eliminate spurious interactions between periodic images in the z -direction, a vacuum layer of 20 Å was introduced between periodic image.

To simulate above-bandgap optical excitation, we used DFT with the constrained occupation scheme, recently developed to study light-induced phenomena in ferroelectric and other materials [38]. In this constrained DFT (cDFT) approach, photoexcitation is modeled by constraining n_{ph} electrons in the conduction band and n_{ph} holes in the valence band during each SCF cycle. The excited electrons and holes are treated as two Fermi-Dirac distributions with their own quasi-Fermi level. A smearing of 0.004 Ha was applied. The system is relaxed under this constraint until convergence is achieved, yielding an SCF solution for the two chemical potentials.

After full relaxation in dark, the FE and the PE phases adopt orthorhombic structures with $Pmm2$ (No. 25) and

$Pmmm$ (No. 47) space group symmetry, respectively, while the AFE phase adopts a monoclinic structure with $P2/m$ (No. 10) space group symmetry. These structures are consistent with previous DFT and experimental studies [25, 28, 39–41]. Vesta illustrations of the final relaxed structures are shown in the Supplemental Materials (SM) [42]. In the FE phase, polarization is induced by the off-center displacement (d) of the Nb atoms along the b -axis. The PE and AFE phases are not polar and have zero total polarization. However, in the AFE phase, the Nb atoms in adjacent cells displace in opposite direction along the b -axis. This gives rise to a null *overall* polarization but non-zero *local* polarizations in the AFE phase. As we will show later, due to the presence of local polar order in the AFE state, its interaction with optical excitation significantly differs from that of the nonpolar PE phase.

III. PHOTO-INDUCED PHASE TRANSITION IN 2D NBOX₂

We start by looking at the photo-induced phase transition in the considered 2D NbOX₂ materials. The total energy of the three phases for NbOCl₂, NbOBr₂ and NbOI₂, as a function of the number of photoexcited carriers concentration is shown on Fig 1. We set the PE phase as the origin of energy at each value of n_{ph} . As stated above, in the dark, the FE is the ground state for all the NbOX₂ materials, followed by the AFE phase and the PE at a much higher energy. As noted in previous studies [25, 28], although the AFE phase is not the ground state, it is a metastable phase very close in energy to the FE phase. As we increase n_{ph} , we notice a gradual reduction in the energy difference between the FE and PE phases but also between the AFE and PE states. As can be seen from Fig 1a, for the 2D NbOCl₂, as we increase n_{ph} , the AFE phase transforms into the PE phase at $n_{ph} = 0.32$ e/f.u. Subsequently at $n_{ph} = 0.36$ e/f.u., the FE phase transforms into the PE. Beyond $n_{ph} = 0.36$ e/f.u., only the PE phase exists. The n_{ph} for the AFE-PE and FE-PE transitions correspond to 2.14×10^{14} cm⁻² and 4.8×10^{14} cm⁻² excited electron-hole pairs with a typical 2 eV pump at $I_0 = 5.0$ mJ.cm⁻² and $I_0 = 6.0$ mJ.cm⁻² fluences, respectively (the details of this estimation is shown in the SM [42]). For the 2D NbOBr₂, the AFE and the FE phases become paraelectric at $n_{ph} = 0.28$ e/f.u and $n_{ph} = 0.32$ e/f.u, respectively. These are equivalent to exciting about 3.4×10^{14} cm⁻² and 3.8×10^{14} cm⁻² electron-hole pairs with the same 2 eV pump at $I_0 = 4.0$ mJ.cm⁻² and $I_0 = 4.50$ mJ.cm⁻² fluences, respectively. And finally for the 2D NbOI₂, the FE and the AFE states are all driven to the PE phase at approximately $n_{ph} = 0.24$ e/f.u corresponding to a density of excited electron-hole pairs of about 1.3×10^{14} cm⁻² with a typical 2.0 eV pump with $I_0 = 3.0$ mJ.cm⁻² as fluence. Beyond $n_{ph} = 0.24$ e/f.u, all the three phases of NbOI₂ evolve as a single PE phase. Using the online FINDSYM utility [43], we also

follow the symmetry of each phase as a function of n_{ph} e/f.u. Consistently with the transition observed in the energy diagram, for each of the three considered 2D allotropes, the FE and the AFE states transform from the $Pmm2$ and $P2/m$, respectively to the centrosymmetric $Pmmm$ space group of the PE phase. We did not, however, observe any transition between the FE and the AFE phases. The transition from FE to PE phases in FE materials has been a subject of previous discussions in the literature. It was found that photoexcited charges can alter polar order in classical perovskite FE materials such as BaTiO₃, PbTiO₃, causing a structural reorganization and suppressing ferroelectric instability, thereby causing transitions from a FE to a PE phase [38, 44]. We follow the evolution of polarization in the FE phases as function of n_{ph} . The uniaxial in-plane polarization in each of the NbOX₂ materials is estimated using the Born effective charges formula $\mathbf{P}_y = S^{-1} \sum_i Z_{yy}^i \mathbf{u}_y$ with Z_{yy}^i is the y component of the Born effective charge tensor (See SM [42] for their values obtained using density functional perturbation theory (DFPT) calculations) of the i atoms, \mathbf{u}_i its displacement with respect to the centrosymmetric position and S the in-plane area of the simulated cell. We also map out the off-center displacement d of two Nb atoms in our cell as function of n_{ph} . This parameter d is known to drive the uniaxial polar behavior in NbOX₂ [25]. The ratio d/d_0 as function of n_{ph} is shown on Fig 2 as full line and filled symbols for the FE phase of each considered 2D NbOX₂, where d_0 is the displacement in dark ($n_{ph} = 0$). The parameter d is decreased by photoexcitation and eventually vanishes at the value of n_{ph} where the FE phase transforms into the centrosymmetric PE phase for each 2D NbOX₂ materials (the polarization as function of n_{ph} is shown the SM [42], follows the same trend and vanishes at the transition point). Previous studies on 2D FE materials such as SnS, SnSe, and similar materials have shown similar polarization behavior [9], but the transition to the PE phase has not been explicitly shown. The effect of illumination on the polarization in the FE phase lets us infer that the observed FE-PE transition is of the same nature as those previously discussed in bulk FE materials [38, 44].

On the other hand, the AFE phase lacks a global polar order. As such the total polarization of the system is always zero. To understand the origin of the light-induced transition from AFE to PE, we also focus on the evolution of the off-center displacement d of Nb atoms in each of the two anti-polar cells of the crystal AFE structure. The ratios d/d_0 , as function of n_{ph} are shown in Fig 2 as open symbols and dashed lines. The trend of d/d_0 indicates that free carriers decrease the off-center displacement of Nb atoms, which, like the local polarization (we estimate the local polarization by considering atoms in one of the polar sublattices of the unit cell [42]), vanishes at the value of n_{ph} where the AFE phase transforms into the PE. This leads to the conclusion that, in the centrosymmetric AFE phase, light also screens the existing “local dipoles” arrangement and thus leads to the transition ob-

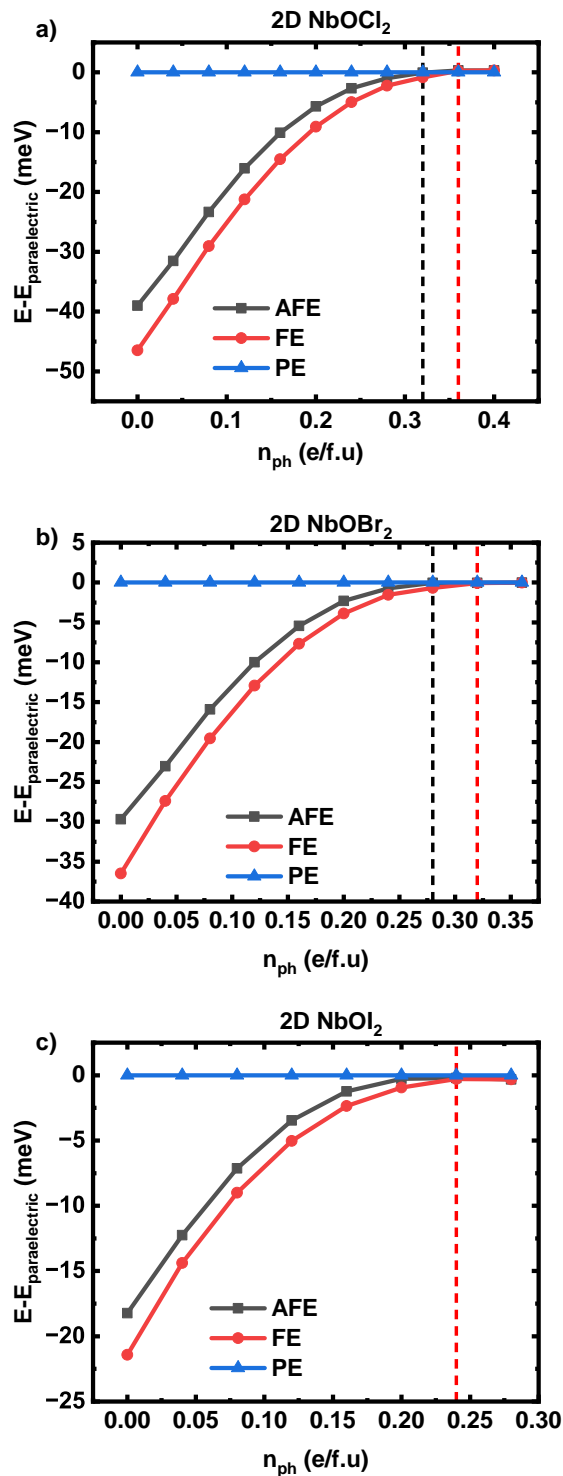


FIG. 1. Energy of the PE, FE and AFE phases of each of the 2D NbOX₂ materials. a) 2D NbOCl₂, b) 2D NbOBr₂ and c) 2D NbOI₂. The energy of the PE phase is set to zero. The black and red dashed lines in a) and b) are guide for the eye to show the transition from AFE to PE and the transition from FE to PE.

served in the energy diagram. This also means that we

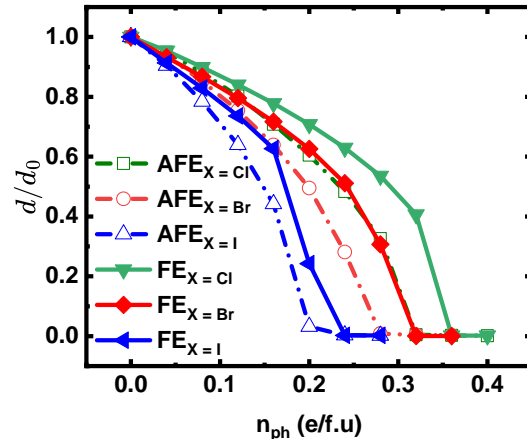


FIG. 2. a) Evolution of the ratio d/d_0 of the FE and AFE phases of each of the 2D NbOX₂ materials as function of n_{ph} : green line for 2D NbOCl₂, red line for 2D NbOBr₂ and blue line for 2D NbOI₂. Dashed lines and open symbols are for the AFE phase. Full lines and filled symbols for the FE phase.

do not observe any FE-to-AFE or AFE-to-FE transition because the effect of illumination on the FE and AFE phases is intrinsically the same, that is screening of local electrical dipoles.

IV. PHOTOSTRICTION IN THE NBOX₂

In this section, we discuss the photostrictive behavior of the 2D layered NbOX₂ phases. In our simulations, we observe that the light-induced strains in the FE, AFE, and PE phases of the considered NbOX₂ are qualitatively similar across structures; i.e., the PE phases exhibit similar qualitative behavior for all X, as do the AFE and FE phases. Consequently, throughout this report, we focus on the results for NbOI₂, referring the reader to the Supplemental Material [42] for data on 2D NbOCl₂ and 2D NbOBr₂ structures. Additionally, we report only the data in the linear regime ($n_{ph} = 0 - 0.16$) e/f.u. for NbOI₂. The remaining data can be found in the SM [42].

As shown on Fig 3a for 2D NbOI₂, in the FE and AFE phases of 2D NbOX₂, light induces an expansion along the nonpolar axis (x) and a compression along the polar/antipolar axis (y) similar to what was observed in early works on 2D FE (SnTe, SnS, GeS) [9, 45]. The same qualitative behavior was also predicted in bulk BiFeO₃ (BFO), BaTiO₃ (BTO) and PbTiO₃ (PTO) where it was found that illumination expands the nonpolar axis while compressing the polar axis [18, 46]. This behavior is, however, in contrast with a recent study that showed that in weakly coupled SrTiO₃/PbTiO₃ superlattices, the polar axis expands upon illumination [47]. As we explained above, the same qualitative behavior of AFE and FE phases can be understood in terms of the screening of

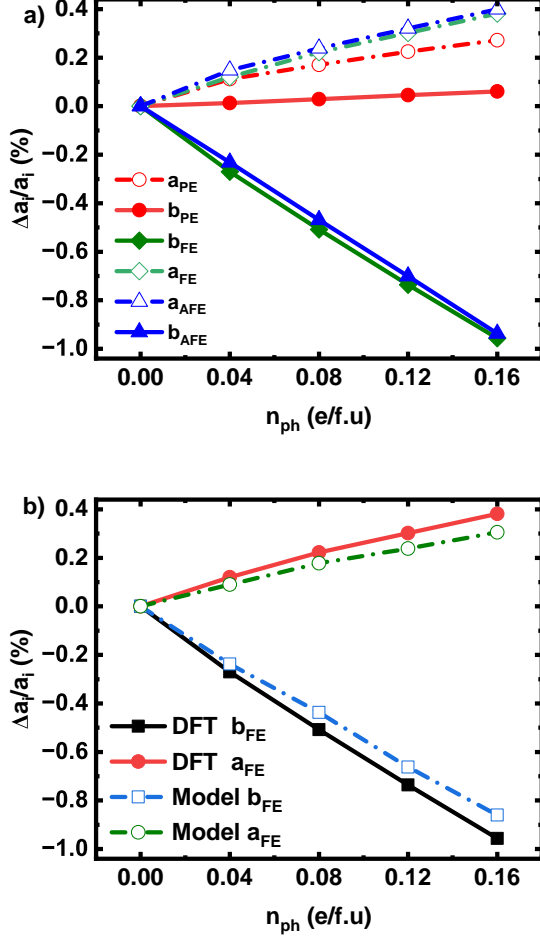


FIG. 3. a) Strain induced in the PE and AFE phases of the 2D NbOI₂ materials as function of $n_{ph} = 0 - 0.16$ e/f.u. Dashed line with open symbols are for strain in the nonpolar axis and full line are the polar/antipolar axis. Blue color for the AFE phase, red color for the PE phase and green color for the FE phase. b) DFT and converse piezoelectric model for the light-induced strains in the FE phases of the 2D NbOI₂

local polar order in the AFE state. Contrary to the observation in the AFE and FE phases, in the PE phase, both lattice lengths increase as we increase the number of photoexcited carrier in our simulations. This shows that the photo-induced strains is dependent on the phases of the layered 2D NbOX₂.

To provide a measure of the photostrictive behavior in these 2D structures that could guide experimental exploration, we extract the slope strains vs photoexcited carrier concentration in the linear regime for each material's considered phases. This slope $\Delta\eta_a/\Delta n_{ph}$ ()/(e/f.u) measures how much the lattice deforms per unit of photoexcited carrier in a formula unit of the material and allows for a better and guided comparison of the predicted photostriction with photostriction in other FE materials in the literature. The results are presented in Table I.

According to Table I, in the linear regime, the FE and AFE phases exhibit nearly the same deformation along the polar/antipolar axis (the in-plane *b*-axis) as well as along the nonpolar axis (the in-plane *a*-axis). As compared to other classical bulk FE materials, the FE phase of NbOX₂ show larger photostrictive behavior than *R3c* BiFeO₃ (-1.5 %/(e/f.u)), *R3m* BaTiO₃ (-0.2 %/(e/f.u)) and PbTiO₃ (-3.1 %/(e/f.u)) [18, 23]. Along the nonpolar axis, they also deform more than PbTiO₃ (-1.0 %/(e/f.u)) [18, 23]. They, however, deform significantly less than 2D SnS (-56.9 %/(e/f.u)) [9] along the polar axis. This comparative behavior is further illustrated in Fig.4.

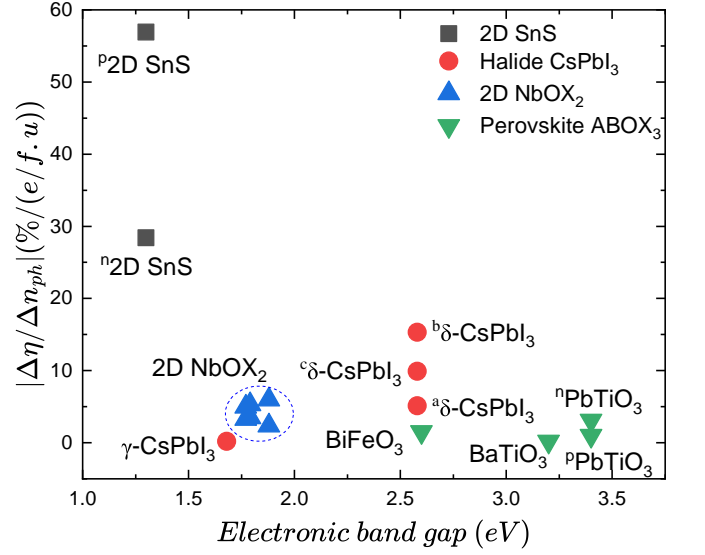


FIG. 4. Absolute values of predicted $\Delta\eta_a/\Delta n_{ph}$ for various materials including classical oxide ferroelectrics, halide perovskites, other 2D materials and the prediction in 2D NbOX₂ materials. The superscript before each element indicates the axis along which the deformation is measured: p represents the polar axis, n denotes the nonpolar axis, and a, b, and c correspond to the a-, b-, and c-axes, respectively

Next, we look at the origin of the photostrictive behavior in the FE phase of these 2D materials. From previous experimental and theoretical studies [5, 9, 10, 15, 18], it has become a general consensus that the inverse piezoelectric effect is a large contribution to the photostriction phenomenon of ferroelectric materials. The excitation of thermalized photoexcited carriers alters polarization in the FE material, which can be thought of as if a light-induced internal electric field was generated in the material, subsequently leading to mechanical deformation through the inverse piezoelectric effect.

In the following, we quantify the converse piezoelectric contribution to the observed photoinduced strains in the FE phases. Using the converse piezoelectric formula and following Refs. [9, 10], the light-induced strains can be

TABLE I. Photostrictive coefficient $\Delta\eta_a/\Delta n_{ph}$ ($\%/(\text{e/f.u.})$) of FE and AFE phases of 2D vdW NbOX₂

	NbOCl ₂		NbOBr ₂		NbOI ₂	
	$\Delta\eta_a/\Delta n_{ph}$	$\Delta\eta_b/\Delta n_{ph}$	$\Delta\eta_a/\Delta n_{ph}$	$\Delta\eta_b/\Delta n_{ph}$	$\Delta\eta_a/\Delta n_{ph}$	$\eta_b/\Delta n_{ph}$
AFE	3.308	-4.903	3.325	-5.168	2.428	-5.856
FE	3.272	-4.966	3.488	-5.314	2.363	-5.944

related to the change in polarization as follows:

$$\eta_i = \frac{d_{i2}}{8\pi\epsilon_0\chi_{2,2}^{2D}} (P(n_{ph} \neq 0) - P(n_{ph} = 0)) \quad (1)$$

with $i = 1, 2$ standing for the a and b axis, d_{12} and d_{22} are the piezoelectric constants of the FE phase and $\chi_{2,2}^{2D}$ the 2D dielectric susceptibilities tensor component along the polar axis. We compute $\chi_{2,2}^{2D}$ and d_{ij} for the FE phase of each NbOX₂, using DFPT as implemented in the Abinit code. Note that the d_{ij} tensor is not a direct output of Abinit. We rather construct it using the relation $e_{ij} = d_{ik}c_{kj}$, from the proper piezoelectric tensor e_{ij} and the elastic constant c_{ij} that are outputs directly from DFPT calculations. The obtained values are plotted on Fig. 3b, showing that the converse piezoelectric accounts for most of the photoinduced strains. Note that the model presented in Eq.1 can also be applied to the AFE phases given the fact that they are locally piezoelectric. To demonstrate that, we adapt Eq.1 to the AFE phase by substituting the FE polarization with the local polarization of the AFE phase's polar sublattice, while retaining the FE piezoelectric coefficient d_{i2} . The results presented in the SM [42] show good agreement with the DFT data for the AFE phase. This is not surprising because, although the local polarization in the AFE differs from that of the FE, the light-induced change in polarization is identical in both phases within the linear regime (See SM [42]). Also, as shown on Fig3a, the light induced strain in both phases are quantitatively similar. These findings mean that, despite the lack of global piezoelectricity, the observed photostrictive behavior in the AFE phase can be attributed to a "local converse piezoelectric

effect."

V. CONCLUSION

In this work, we present first-principles investigation of the impact of optical excitation on the layered 2D NbOX₂ materials. We demonstrate that illumination not only induces a FE to PE transition in these 2D systems but also an AFE to PE transition. Additionally, we present results on the photostrictive behavior in 2D NbOX₂, showing an enhanced behavior compared to bulk FE such as BiFeO₃, BaTiO₃ and PbTiO₃. Notably, this significant photostrictive response can be realized at carrier densities that are experimentally accessible. Our study establishes 2D NbOX₂ as promising candidates for applications in remote actuation, sensing, and non-volatile optoelectronic devices.

ACKNOWLEDGMENTS

This work is supported by the Grant No. MURI ETHOS W911NF-21-2-0162 from Army Research Office (ARO), the ARO Grant No. W911NF-21-1-0113, and the Vannevar Bush Faculty Fellowship (VBFF) Grant No. N00014-20-1-2834 from the Department of Defense. C.P. acknowledges support from the Air Force Office of Scientific Research through Award No. FA9550-24-1-0263. This research is also supported by the Arkansas High Performance Computing Center, which is funded through multiple National Science Foundation grants and the Arkansas Economic Development Commission.

-
- [1] B. C. Sekhar, B. Dhanalakshmi, B. S. Rao, S. Ramesh, K. V. Prasad, P. Rao, and B. P. Rao, Piezoelectricity and its applications, *Multifunct. Ferroelectr. Mater* **71** (2021).
 - [2] H. Shaukat, A. Ali, S. Bibi, S. Mehmood, W. A. Altabey, M. Noori, and S. A. Kouritem, Piezoelectric materials: Advanced applications in electro-chemical processes, *Energy Reports* **9**, 4306 (2023).
 - [3] D. A. Berlincourt, D. R. Curran, H. Jaffe, *et al.*, Piezoelectric and piezomagnetic materials and their function in transducers, *Physical Acoustics: Principles and Methods* **1**, 202 (1964).
 - [4] S. Mohith, A. R. Upadhy, K. P. Navin, S. Kulkarni, and M. Rao, Recent trends in piezoelectric actuators for

- precision motion and their applications: A review, *Smart Materials and Structures* **30**, 013002 (2020).
- [5] B. Kundys, Photostrictive materials, *Appl. Phys. Rev.* **2**, 011301 (2015).
- [6] H. Finkelmann, E. Nishikawa, G. Pereira, and M. Warner, A new opto-mechanical effect in solids, *Phys. Rev. Lett.* **87**, 015501 (2001).
- [7] P. Poosanaas, K. Tonooka, and K. Uchino, Photostrictive actuators, *Mechatronics* **10**, 467 (2000).
- [8] D. Sun and L. Tong, Modeling of wireless remote shape control for beams using nonlinear photostrictive actuators, *International Journal of Solids and Structures* **44**, 672 (2007).

- [9] R. Haleoot, C. Paillard, T. P. Kaloni, M. Mehboudi, B. Xu, L. Bellaiche, and S. Barraza-Lopez, Photostrictive two-dimensional materials in the monochalcogenide family, *Phys. Rev. Lett.* **118**, 227401 (2017).
- [10] C. Paillard, S. Prosandeev, and L. Bellaiche, Ab initio approach to photostriction in classical ferroelectric materials, *Phys. Rev. B* **96**, 045205 (2017).
- [11] C. Paillard, X. Bai, I. C. Infante, M. Guennou, G. Geneste, M. Alexe, J. Kreisel, and B. Dkhil, Photovoltaics with ferroelectrics: Current status and beyond, *Adv. Mater.* **28**, 5153 (2016).
- [12] S. Matzen, L. Guillemot, T. Maroutian, S. K. Patel, H. Wen, A. D. DiChiara, G. Agnus, O. G. Shpyrko, E. E. Fullerton, D. Ravelosona, *et al.*, Tuning ultrafast photoinduced strain in ferroelectric-based devices, *Advanced Electronic Materials* **5**, 1800709 (2019).
- [13] L. Gao, C. Paillard, and L. Bellaiche, Photoinduced control of ferroelectricity in hybrid-improper ferroelectric superlattices, *Phys. Rev. B* **107**, 104109 (2023).
- [14] B. Kundys, M. Viret, C. Meny, V. Da Costa, D. Colson, and B. Doudin, Wavelength dependence of photoinduced deformation in BiFeO_3 , *Phys. Rev. B* **85**, 092301 (2012).
- [15] B. Kundys, M. Viret, D. Colson, and D. O. Kundys, Light-induced size changes in BiFeO_3 crystals, *Nature materials* **9**, 803 (2010).
- [16] H. Wen, P. Chen, M. P. Cosgriff, D. A. Walko, J. H. Lee, C. Adamo, R. D. Schaller, J. F. Ihlefeld, E. M. Dufresne, D. G. Schlom, *et al.*, Electronic origin of ultrafast photoinduced strain in BiFeO_3 , *Phys. Rev. Lett.* **110**, 037601 (2013).
- [17] D. Schick, M. Herzog, H. Wen, P. Chen, C. Adamo, P. Gaal, D. G. Schlom, P. G. Evans, Y. Li, and M. Bargheer, Localized excited charge carriers generate ultrafast inhomogeneous strain in the multiferroic BiFeO_3 , *Phys. Rev. Lett.* **112**, 097602 (2014).
- [18] C. Paillard, B. Xu, B. Dkhil, G. Geneste, and L. Bellaiche, Photostriction in ferroelectrics from density functional theory, *Phys. Rev. Lett.* **116**, 247401 (2016).
- [19] R. Gu, V. Juvé, C. Laulhé, H. Bouyanfif, G. Vaudel, A. Poirier, B. Dkhil, P. Hollander, C. Paillard, M. C. Weber, *et al.*, Temporal and spatial tracking of ultrafast light-induced strain and polarization modulation in a ferroelectric thin film, *Science Advances* **9**, eadi1160 (2023).
- [20] M. Nakano and T. Ikeda, Photomechanics: directed bending of a polymer film by light, *Nature* **425**, 145 (2003).
- [21] J. R. Buschert and R. Colella, Photostriction effect in silicon observed by time-resolved x-ray diffraction, *Solid state communications* **80**, 419 (1991).
- [22] Y. Zhou, L. You, S. Wang, Z. Ku, H. Fan, D. Schmidt, A. Rusydi, L. Chang, L. Wang, P. Ren, *et al.*, Giant photostriction in organic-inorganic lead halide perovskites, *Nature communications* **7**, 11193 (2016).
- [23] C. Paillard and L. Bellaiche, Light: A new handle to control the structure of cesium lead iodide, *Phys. Rev. B* **107**, 054107 (2023).
- [24] B. Peng, D. Bennett, I. Bravić, and B. Monserrat, Tunable photostriction of halide perovskites through energy dependent photoexcitation, *Phys. Rev. Mat.* **6**, L082401 (2022).
- [25] Y. Jia, M. Zhao, G. Gou, X. Cheng Zeng, and J. Li, Niobium oxide dihalides NbOX_2 : a new family of two-dimensional van der Waals layered materials with intrinsic ferroelectricity and antiferroelectricity, *Nanoscale Horizons* **4**, 1113 (2019).
- [26] J. Rijnsdorp and F. Jellinek, The crystal structure of niobium oxide diiodide NbOI_2 , *Journal of the Less Common Metals* **61**, 79 (1978).
- [27] C. Liu, X. Zhang, X. Wang, Z. Wang, I. Abdelwahab, I. Verzhbitskiy, Y. Shao, G. Eda, W. Sun, L. Shen, and K. P. Loh, Ferroelectricity in niobium oxide dihalides NbOX_2 ($x = \text{Cl}, \text{I}$): A macroscopic to microscopic scale study, *ACS Nano* **17**, 7170 (2023).
- [28] Y. Wu, I. Abdelwahab, K. C. Kwon, I. Verzhbitskiy, L. Wang, W. H. Liew, K. Yao, G. Eda, K. P. Loh, L. Shen, and S. Y. Quek, Data-driven discovery of high performance layered van der Waals piezoelectric NbOI_2 , *Nat Commun* **13**, 1884 (2022).
- [29] Q. Guo, X.-Z. Qi, L. Zhang, M. Gao, S. Hu, W. Zhou, W. Zang, X. Zhao, J. Wang, B. Yan, M. Xu, Y.-K. Wu, G. Eda, Z. Xiao, S. A. Yang, H. Gou, Y. P. Feng, G.-C. Guo, W. Zhou, X.-F. Ren, C.-W. Qiu, S. J. Pennycook, and A. T. S. Wee, Ultrathin quantum light source with van der waals NbOCl_2 crystal, *Nature* **613**, 53 (2023).
- [30] Y. Wang, Y. Wu, and M. Sun, Indirect and direct electronic transitions and electron transport properties of van der Waals NbOCl_2 , *Phys. Chem. Chem. Phys.* **26**, 22518 (2024).
- [31] I. Abdelwahab, B. Tilmann, Y. Wu, D. Giovanni, I. Verzhbitskiy, M. Zhu, R. Berté, F. Xuan, L. d. S. Menezes, G. Eda, T. C. Sum, S. Y. Quek, S. A. Maier, and K. P. Loh, Giant second-harmonic generation in ferroelectric NbOI_2 , *Nat. Photon.* **16**, 644 (2022).
- [32] G. Zhang, T. Zhang, Q. Xia, Q. Chen, and J. Wang, Enhanced Carrier Lifetime and Mobility in Monolayer NbOI_2 , *J. Phys. Chem. Lett.* **15**, 10032 (2024).
- [33] N. Zhang, N. Li, L. Wang, M. Sun, and J. Wang, Linear and nonlinear optical absorption of 2d monolayer NbOCl_2 , *Journal of Molecular Structure* **1299**, 137064 (2024).
- [34] Z. Zhang, X. Di, C. Paillard, L. Bellaiche, and Z. Jiang, Giant electro-optic and elasto-optic effects in ferroelectric $\{\text{NbOI}\}_2$, *Phys. Rev. B* **110**, L100101 (2024).
- [35] A. H. Romero, D. C. Allan, B. Amadon, G. Antonius, T. Applencourt, J. B. L. Baguet, F. Bottin, J. Bouchet, E. Bousquet, F. Bruneval, G. Brunin, M. C. D. Caliste, J. Denier, C. Dreyer, P. Ghosez, M. Giantomassi, Y. Gillet, O. Gingras, D. R. Hamann, G. Hautier, F. Jollet, G. Jonard, A. Martin, H. P. C. Miranda, F. Naccarato, G. Petretto, N. A. Pike, V. Planes, S. Prokhorenko, T. Rangel, F. Ricci, G. M. Rignanese, M.ROY, M. Stengel, M. Torrent, M. J. van Setten, B. V. Troeye, M. J. Verstraete, J. Wiktor, J. W. Zwanziger, and X. Gonze, Abinit: Overview and focus on selected capabilities, *J. Chem. Phys.* **152**, 124102 (2020).
- [36] D. Hamann, Optimized norm-conserving vanderbilt pseudopotentials, *Physical Review B—Condensed Matter and Materials Physics* **88**, 085117 (2013).
- [37] J. P. Perdew, K. Burke, and M. Ernzerhof, Generalized gradient approximation made simple, *Physical review letters* **77**, 3865 (1996).
- [38] C. Paillard, E. Torun, L. Wirtz, J. Íñiguez, and L. Bellaiche, Photoinduced phase transitions in ferroelectrics, *Phys. Rev. Lett.* **123**, 087601 (2019).
- [39] H. Wang, Q. Chen, Y. Cao, W. Sang, F. Tan, H. Li, T. Wang, Y. Gan, D. Xiang, and T. Liu, Anisotropic

- Strain-Tailoring Nonlinear Optical Response in van der Waals NbOI₂, *Nano Lett.* **24**, 3413 (2024).
- [40] G. Zhang, Q. Chen, and J. Wang, Structural phase transition and electronic properties of two-dimensional NbOI_2 , *Phys. Rev. B* **109**, 184103 (2024).
- [41] M. A. Mohebpour, S. I. Vishkayi, V. Vitale, N. Seriani, and M. B. Tagani, Origin and properties of the flat band in monolayer NbOCl₂, *Phys. Rev. B* **110**, 035429 (2024).
- [42] See supplemental material at [url] for the additional data., .
- [43] H. T. Stokes and D. M. Hatch, Findsymb: program for identifying the space-group symmetry of a crystal, *Journal of Applied Crystallography* **38**, 237 (2005).
- [44] V. Krapivin, M. Gu, D. Hickox-Young, S. W. Teitelbaum, Y. Huang, G. De La Peña, D. Zhu, N. Sirica, M.-C. Lee, R. Prasankumar, *et al.*, Ultrafast suppression of the ferroelectric instability in ktao₃, *Physical review letters* **129**, 127601 (2022).
- [45] D. Luo, B. Zhang, E. J. Sie, C. M. Nyby, Q. Fan, X. Shen, A. H. Reid, M. C. Hoffmann, S. Weathersby, J. Wen, X. Qian, X. Wang, and A. M. Lindenberg, Ultrafast optomechanical strain in layered GeS, *Nano Lett.* **23**, 2287 (2023).
- [46] C. Paillard, S. Prosandeev, and L. Bellaiche, Ab initio approach to photostriction in classical ferroelectric materials, *Physical Review B* **96**, 045205 (2017).
- [47] C. Dansou, C. Paillard, and L. Bellaiche, Tuning photostriction in pbtio₃/srtio₃ superlattices: An ab initio study, *Physical Review B* **110**, 224303 (2024).